Petrology, geochemistry (Ore deposits)

Metallogeny of the Paramillos de Uspallata Pb–Zn–Ag vein deposit in the Cuyo Rift Basin, Argentina

Nora A. Rubinstein [a],*, Silvia I. Carrasquero [b], Anabel L.R. Gómez [a], Ana P. Orellano Ricchetti [a], María C. D'Annunzio [c]

[a] *Instituto de Geociencias Básicas, Aplicadas y Ambientales de Buenos Aires (Universidad de Buenos Aires–CONICET), Intendente Güiraldes 2160, Pabellón II, Piso 1, Ciudad Autónoma de Buenos Aires, Buenos Aires, Argentina*
[b] *Facultad de Ciencias Naturales y Museo, Universidad Nacional de La Plata, La Plata, Argentina*
[c] *Instituto Geológico del Sur (Universidad Nacional del Sur–CONICET), Bahía Blanca, Argentina*

A B S T R A C T

The Paramillos de Uspallata deposit, previously considered as genetically linked to a Miocene porphyry deposit, is located in the Mesozoic Cuyo Basin, which was formed during the beginning of the break-up of Gondwana. In the present study, both previous information and new geological, mineralogical, and isotopic data allowed outlining a new descriptive model for this deposit. Stratigraphic and structural controls allowed considering this deposit as contemporaneous with the Mesozoic rifting, with the mineralization resulting from a Pb–Zn stage followed by an Ag–Cu–Pb stage. The hydrothermal fluids were found to have low temperature and low to moderate salinity, and to result from the mixing between metamorphic and meteoric fluids, with the lead sourced by the igneous Paleozoic basement and the sulfur partly derived from a magmatic source. These characteristics allow describing Paramillos de Uspallata as Pb–Zn–Ag veins hosted in clastic sedimentary sequences genetically linked to a rift basin and redefining it as detachment-related mineralization.

© 2018 Académie des sciences. Published by Elsevier Masson SAS. All rights reserved.

1. Introduction

Silver–lead–zinc veins hosted in clastic sedimentary sequences (CSS Pb–Zn–Ag veins) form a distinct class of mineral deposits with a distinctive mineralogy, associated with crustal-scale faults (Beaudoin and Sangster, 1992). Several examples of this class of deposits have been documented around the world, in the Kokanee Range (Beaudoin and Sangster, 1992), Keno Hill district (Lynch et al., 1990) and Purcell Basin (Paiement et al., 2012) in Canada; the Freiberg district (Baumann, 1994) and Harz Mountains (Lüders and Möller, 1992) in Germany; the

Coeur d'Alene district (Fleck et al., 2002; Leach et al., 1998; Lydon, 2007) in the USA; the Pribram district (Zàk and Dobes, 1991) in the Czech Republic; and the Pumahuasi district in Argentina (Segal et al., 1999). Based on a worldwide review, Beaudoin and Sangster (1992) proposed a descriptive model for CSS Pb–Zn–Ag veins and discussed different alternative models for their genesis.

The Paramillos de Uspallata Pb–Zn–Ag vein deposit (32°28′29.6″S; 69°08′46″W) is hosted in the northern part of the Cuyo Basin, which extends along ~60,000 km² between 31° and 36° S in the Andean Cordillera (Fig. 1). This basin is the largest of the Triassic basins of Southwest Gondwana in Argentina related to a generalized extension linked to the collapse of the Permian orogen and the beginning of the Mesozoic Gondwana break-up (Legarreta and Uliana, 1996; Tankard et al., 1995; Uliana et al., 1989).

---

* Corresponding author.
  E-mail addresses: narubinstein@gmail.com, nora@gl.fcen.uba.ar (N.A. Rubinstein).
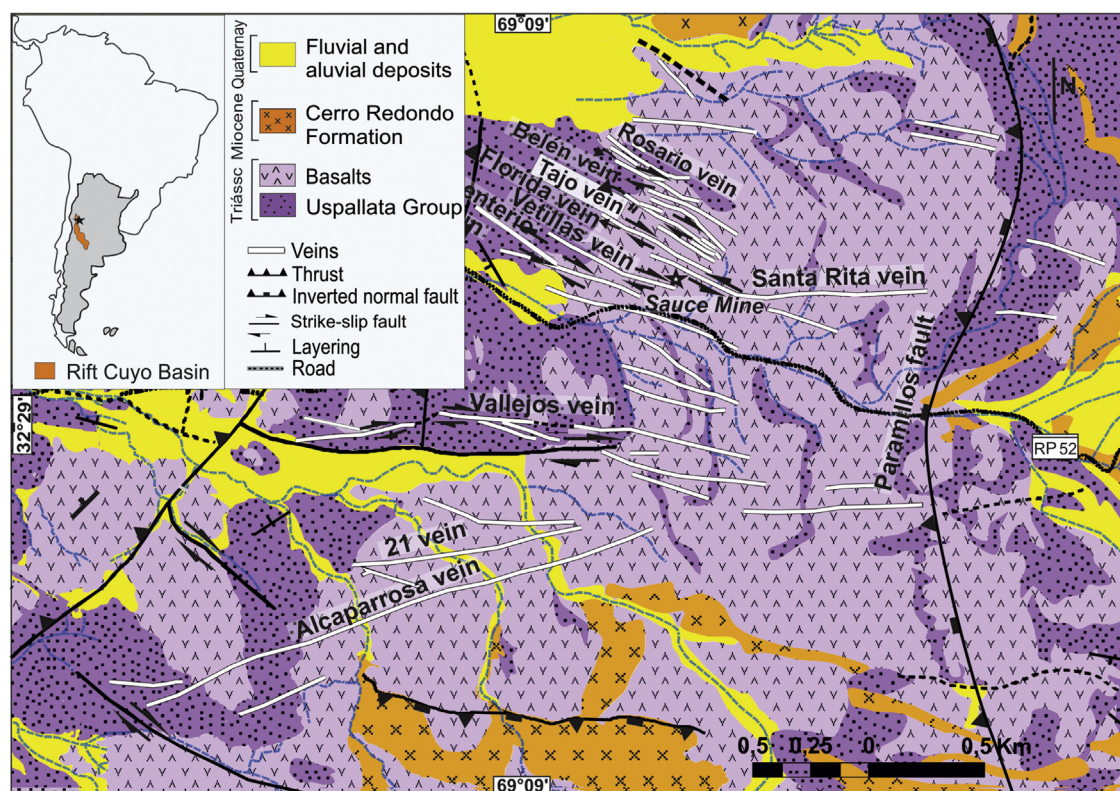
Fig. 1. Location of the Cuyo Basin and geological sketch of the Paramillos de Uspallata vein deposit area. Star: study area.

From the 17th century until the early 1980s, the Paramillos de Uspallata Pb–Zn–Ag vein-type deposit was discontinuously mined, producing nearly 414,000 t of ore at ∼2.5% Pb, 3.5% Zn and 475 g/t Ag (Lavandaio and Fusari, 1999). At present, there are only a few intense oxidized outcropping veins, and only ∼1,200 m of the ∼20,000 m of underground documented galleries are currently accessible. It is currently a geopark where it is possible to visit the ruins of the old miner town and access the underground mining works. Although it is the oldest mine in Argentina, there are few previous studies about this deposit. These include the description of the mining works (Rayces, 1949), some specific fluid inclusions and isotope studies (Garrido et al., 2001), and limited geochemical work (Lavandaio and Fusari, 1999). Thus, its genesis still remains controversial.

The aim of this study was to build a new descriptive model of the Paramillos de Uspallata Pb–Zn–Ag vein deposit based on both new and existing metallogenic information, particularly mineralogical, petrographic, and isotopic data, in order to elucidate its genesis and provide insights into a class of mineral deposit whose genesis still remains partly unresolved.

2. Geological setting

2.1. Regional geology

The Cuyo Basin is a passive rift system located in western Argentina (Fig. 1). It is composed of asymmetric half-grabens controlled by preexisting zones of weak-

nesses in the basement related to the ancient Gondwanan sutures separated by transfer faults or intrabasinal highs that led to different depocenters. The basin infill consists of up to 3700 m of a volcano-sedimentary sequence overlying a basement consisting of Paleozoic sedimentary rocks and Permian–Triassic volcanics (Choiyoi Group). The lower part of this sequence is composed of coarse-grained alluvial, fluvial, lacustrine, deltaic, and volcaniclastic deposits of the Early to Mid-Triassic synrift stage, a stage characterized by tectonic subsidence related to the activity of the main fracture systems along the active flank of the half-grabens (Spalletti, 1999). During this synrift phase, tholeiitic to slightly alkaline basalts with moderately steep rare-earth element patterns and mantle-like isotopic ratios emplaced during the Middle Triassic (∼235 Ma) (Massabie, 1986; Ramos and Kay, 1991; Rocher et al., 2015). The chemistry of these basalts suggests relatively low degrees of melting (4 to 5%), which is consistent with the comparatively narrow width of the Cuyo Basin (Ramos and Kay, 1991). The synrift deposits are overlaid by Middle to early Late Triassic dominant fluvial-lacustrine successions deposited under thermal-tectonic subsidence conditions (sag phase) of the basin. The upper part of these sag deposits is composed of Late Triassic alluvial–fluvial successions related to tectonic subsidence reactivation. The thermal relaxation of the basin finished with the flexural subsidence of the lithosphere triggered by the Andean Orogeny during the Cenozoic (Barredo, 2012; Spalletti, 1999).

By the latest Early Miocene, the collision of the Juan Fernández Ridge resulted in the shallowing of the subducting plate between 28 and 33°S, which was accompanied by a change in the deformation regime from transpressional to compressional, crustal thickening, eastward frontal arc migration, and a change in the geochemical signature of the magmatism (Kay and Mpodozis, 2002; Yáñez et al., 2001). Synchronously with the initiation of the compressional deformation and arc migration, a dominant andesitic magmatism erupted in a broadened arc that extended into the western Precordillera (Carrasquero et al., 2017).

2.2. Deposit-scale geology

The Paramillos de Uspallata vein-system deposit is hosted in the Triassic synrift volcano-sedimentary sequence locally named Uspallata Group (Fig. 1), which includes the Paramillos and Agua de la Zorra Formations. The Paramillos Formation is a volcano-sedimentary unit which hosts an *in situ* fossil forest of conifers and corystosperms (Brea et al., 2009). It is composed of sandstones, tuffaceous sandstones, shales, mudstones, and tuffs, which were deposited in a meandering fluvial system (Brea et al., 2009) during the upper Middle Triassic (~239–230 Ma, Spalletti et al., 2008). The overlying Agua de la Zorra Formation consists mainly of bituminous shales and marls with minor interbedded sandstones and mudstones, which were deposited in a fluvial shallow lacustrine environment with episodic eruptive events (Brea et al., 2009; Cortés et al., 1997).

Interbedded with the Paramillos and Agua de la Zorra Formations, there are basaltic lava flows, locally with vesicles filled with carbonate and minor quartz, and subordinate basaltic sills and dykes. The volcanics have porphyritic texture with plagioclase, clinopyroxene (augite) and scarce olivine phenocrysts in an intergranular to intersertal groundmass composed mainly of plagioclase with variable augite and abundant magnetite. These mafic rocks show variable alteration depending on their vesicularity and their primary glass content with their igneous texture widely retained. The alteration paragenesis is dominated by ubiquitous chlorite along with carbonate and titanite, with minor epidote, prehnite and pumpellyite as well as very scarce albite, actinolite, quartz, and zeolites. The alteration minerals occur as a replacement of interstitial areas and primary minerals and infilling of vesicles and veins. This paragenesis corresponds to very low-grade metamorphism in the prehnite–pumpellyite facies in metabasites.

The Triassic sequence is intruded by arc andesitic subvolcanic rocks (Cerro Redondo Formation, Fig. 1) of latest Early Miocene age (~20–16 Ma, Kay et al., 1991; Massabie, 1986). Cu–Mo porphyry-type and Au-epithermal-type deposits are spatially and genetically associated with these Miocene magmatic rocks (Carrasquero et al., 2011; Navarro, 1972).

3. Zn–Pb–Ag mineralization

The Paramillos de Uspallata deposit includes 33 subvertical veins with predominantly NW and WNW and subordinate WSW strikes hosted in the volcano-sedimentary Triassic sequence (Figs. 1 and 2a). These veins are of up to ~2 m thick and extend for up to ~2500 m along strike and consist of sulfides and sulfosalts and siderite as the main gangue mineral, typically displaying crustiform, cockade, and breccia textures (Fig. 2b). The wall-rock alteration surrounding the veins is moderate to intense and includes pervasive sericitization and carbonatization and veinlet-type silicification.

Ore petrography studies have shown that the mineralization consists of an intergrowth of galena and sphalerite with chalcopyrite disease, minor chalcopyrite, and scarce pyrite in a siderite with minor quartz gangue. These sulfides are variably replaced by a mineral of the tetrahedrite–tennantite series, which is, in turn, variably replaced by tabular and acicular sulfosalt aggregates (Ss1 and Ss2, see Fig. 2c). Late discontinuous veinlets of arsenopyrite and marcasite in a quartz gangue cut the above-mentioned ore mineral assemblage.

4. Results

4.1. Mineral chemistry and ore paragenetic sequence

The sulfides and sulfosalts of four vein samples were chemically analyzed with a Cameca SX-100 Electron Probe Microanalyzer (EPM) in the Research Centre for Physical and Environmental Science, Open University, UK. The analytical conditions were 20 kV for the accelerating voltage, 20 nA for the beam current and a beam diameter of 2, 5, and 10 μm. The standard reference materials used for calibration were S (Kα/Sp3), Ag (Lα/Sp5), Fe (Kα/Sp1), Mn (Kα/Sp1), Cu (Kα/Sp3), Zn (Kα/Sp1), Cd (Lα/Sp5), Hg (Lα/Sp3), (Pb Mα/Sp5), Sb (Lα/Sp4), As (Kα/Sp1), and Bi (Mα/Sp4). The representative composition and the structural formula of the mineral phases analyzed are presented in Table 1.

The EPM analyses and back-scattered electron images (Fig. 3a) of galena showed very small pyrargyrite inclusions. In addition, they showed low and erratic contents of Cu (up to ~0.4%), Bi (~1%), Sb (up to ~0.23%), and Ag (up to 2%), and traces of Fe, Hg, and Zn. The contents of Ag could be due to the presence of sub-microscopic inclusions of pyrargyrite. Sphalerite showed variable Fe (~0.8–8%) and low Au (~0.4%) contents, whereas chalcopyrite showed a homogeneous composition with low and erratic contents of Zn (up to ~1%) and traces of Ag, Pb, As, and Bi.

The structural formula of the mineral identified by ore petrography as tetrahedrite–tennantite (Table 1) revealed that it is a member of the freibergite–tetrahedrite series (see Riley, 1974). This mineral displayed variable contents of Ag (~20 to 27%) heterogeneously distributed in the crystals (Fig. 3b) and very low contents of As (< 0.4%). The EPM analyses also showed that the tabular and acicular sulfosalt aggregates that replace the freibergite–tetrahedrite are composed of boulangerite and owyheeite (Fig. 3c). Boulangerite is typically stoichiometric and has low contents of Bi (~0.7%), whereas owyheeite has a chemical composition that fits with that obtained by Moëlo et al. (1984) for owyheeites from different ore deposits around
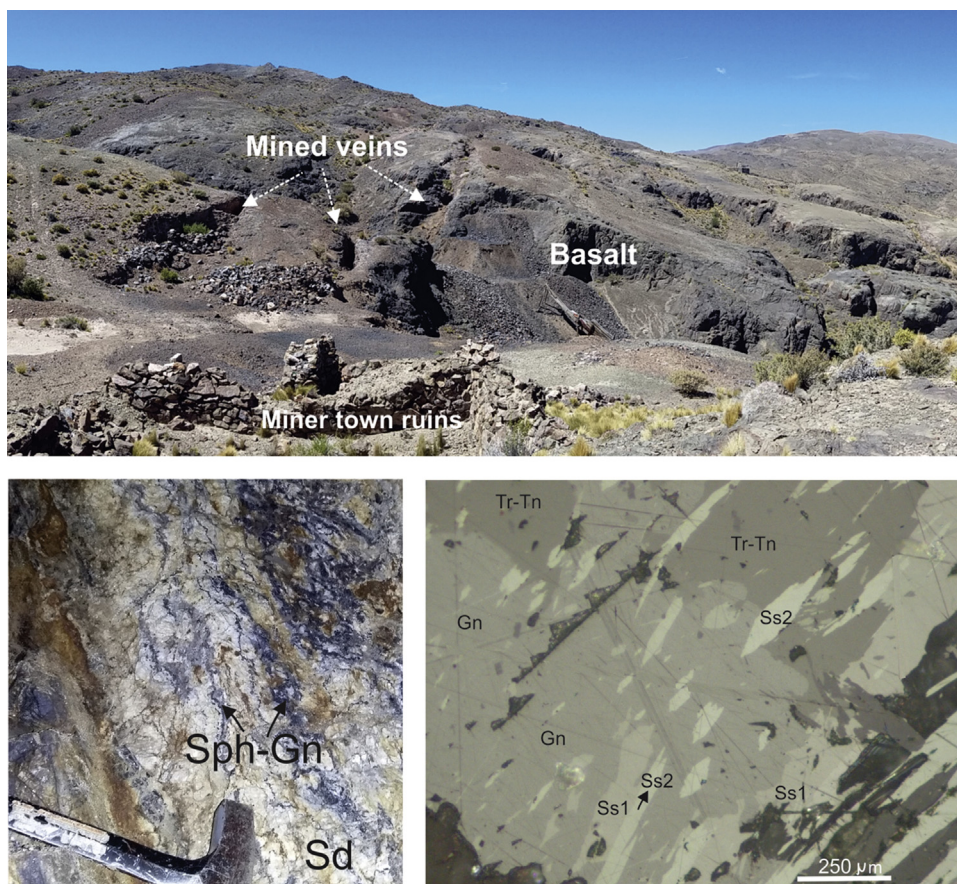
Fig. 2. A. Mined veins hosted by the Triassic basalts. B. Vein consisting of siderite (Sd) and sulfides (mainly galena, Gn and sphalerite, Sph) displaying characteristic crustiform texture. C. Galena (Gn) replaced by a mineral of the tetrahedrite–tennantite series (Tt–tn), which is variably replaced by different sulfosalts (Ss1 and Ss2).

the world, but with higher Ag (∼9–10% instead of ∼5–7%), similar to that reported for Rivertree, New South Wales (Lawrence, 1962). The images show that marcasite occurs as fine aggregates with banded texture (probable after melnikovite, see Fig. 3d). Finally, arsenopyrite displays a homogeneous composition with traces of Ag, Mn, Au, Pb, and Bi. Ore petrographic studies plus mineral chemistry results allowed establishing the paragenetic sequence shown in Fig. 4.

4.2. Oxygen and carbon isotopes

The results of oxygen isotope analyses performed on quartz and oxygen and those of carbon isotope analyses performed on siderite are reported in Table 2 along with data from Garrido et al. (2001).

The quartz concentrates were reacted with BrF5 according to the method of Clayton and Mayeda (1963) at the Stable Isotope Laboratory of Université Laval, Québec, Canada, and the CO_2 was analyzed by Isotope-ratio mass spectrometry (IRMS) at the Geological Survey of Canada, Québec. The accuracy and precision of the ^{18}O values were verified by analysis of NBS-28. Isotope ratios are reported in the δ-notation relative to V-SMOW with a precision better than 0.2‰.

Siderite was reacted with 100% phosphoric acid at 25 °C and the CO_2 obtained was analyzed by IRMS, using an internal standard periodically calibrated with the International NBS-19 (calcite) standard at the ACTLABS Laboratories, Canada. Isotope ratios are reported in the δ-notation relative to V-SMOW for oxygen and PDB for carbon, with a precision better than 0.2‰ for ^{13}C and ^{18}O.

In general, the $\delta^{18}O$ values of the hydrothermal fluid equilibrated with siderite (from 4.579 to 10.278‰, see Table 2) were within the oxygen isotopic composition range of magmatic and deep-seated (metamorphic) waters (∼5.5 to 9‰ and ∼5 to 25‰ respectively, see Taylor, 1974). This is consistent with the $\delta^{13}C$ values obtained (Table 2), which were also in the range of those of magmatic and deep-seated fluids (∼–9 to –4‰, see Zheng and Hoefs, 1993). Besides, the $\delta^{18}O$ values of the fluid equilibrated with quartz were lighter than those of siderite and broadly scattered to the left (from ∼5.3 to –1‰, see Table 2), suggesting a variable involvement of meteoric waters characteristically with $\delta^{18}O < 0$ (see Taylor, 1974).

4.3. Lead isotopes

Galena from three different veins and two samples of the Mesozoic basaltic host rocks were analyzed for Pb

Table 1
Representative analyses (by means of Electron Probe Microanalyzer) of sulfides and sulfosalts from the Paramillos de Uspallata deposit.

	Galena		Pyrargyrite	Sphalerite		Arsenopyrite	Chalcopyrite		Marcasite		Boulangerite		Owyheeite		Tetrahedrite-Freibergite	
S (wt%)	14.90	13.77	16.86	32.50	32.46	20.93	34.18	33.66	52.89	52.29	18.71	19.07	19.58	20.29	20.89	22.50
Ag	1.99	0.00	57.34	0.03	0.01	0.03	0.00	0.11	0.03	0.15	0.00	0.00	10.00	9.04	27.55	20.78
Fe	0.12	0.09	0.00	0.85	8.40	34.93	29.15	28.53	45.32	45.42	0.01	0.04	0.10	0.08	3.77	5.54
Mn	0.00	0.00	0.00	0.00	0.03	0.00	0.08	0.00	0.03	0.17	0.00	0.01	0.00	0.00	0.01	0.00
Au	0.00	0.00	0.00	0.43	0.44	0.00	0.00	0.00	0.00	0.19	0.00	0.00	0.00	0.00	0.00	0.08
Cu	0.44	0.01	0.02	0.06	0.00	0.01	33.60	33.11	0.02	0.02	0.01	0.00	0.16	0.15	18.10	22.32
Zn	0.01	0.11	0.13	63.72	54.59	0.42	0.02	1.17	0.44	0.03	0.00	0.11	0.00	0.00	2.09	1.03
Cd	0.00	0.00	0.00	0.37	0.01	0.00	0.00	0.00	0.00	0.00	0.00	0.00	0.00	0.00	0.00	0.00
Hg	0.09	0.00	0.06	0.00	0.00	0.06	0.00	0.04	0.00	0.03	0.00	0.02	0.04	0.04	0.07	0.03
Pb	83.23	84.67	0.00	0.08	0.08	0.06	0.00	0.10	0.25	0.28	55.90	55.45	39.77	38.39	0.00	0.03
Sb	0.01	0.23	19.72	0.11	0.01	0.49	0.00	0.00	0.00	0.03	24.13	24.75	29.74	31.37	25.95	26.96
As	0.00	0.00	4.41	0.59	1.08	41.96	0.10	0.24	0.00	0.00	0.00	0.00	0.00	0.00	0.27	0.36
Bi	0.00	1.11	0.17	0.07	0.11	0.06	0.12	0.11	0.19	0.16	0.73	0.75	0.56	0.55	0.13	0.04
Sum	100.78	100.00	98.71	98.80	97.23	98.95	97.24	97.07	99.18	98.77	99.48	100.20	99.95	99.91	98.84	99.67
	2 atoms		7 atoms	2 atoms		3 atoms	4 atoms		3 atoms		20 atoms		52 atoms		30 atoms	
S	1.04	1.01	2.87	1.00	1.00	1.06	2.01	2.00	2.00	1.99	11.06	11.10	27.69	28.21	12.95	13.26
Ag	0.04	0.00	2.90	0.00	0.00	0.00	0.00	0.00	0.00	0.00	0.00	0.00	4.20	3.73	5.08	3.64
Fe	0.00	0.00	0.00	0.01	0.15	1.01	0.98	0.97	0.99	0.99	0.00	0.01	0.08	0.07	1.34	1.88
Mn	0.00	0.00	0.00	0.00	0.00	0.00	0.00	0.00	0.00	0.00	0.00	0.00	0.00	0.00	0.00	0.00
Au	0.00	0.00	0.00	0.00	0.00	0.00	0.00	0.00	0.00	0.00	0.00	0.00	0.00	0.00	0.00	0.01
Cu	0.02	0.00	0.00	0.00	0.00	0.00	1.00	0.99	0.00	0.00	0.00	0.00	0.12	0.11	5.66	6.64
Zn	0.00	0.00	0.01	0.97	0.83	0.01	0.00	0.03	0.01	0.00	0.00	0.03	0.00	0.00	0.64	0.30
Cd	0.00	0.00	0.00	0.00	0.00	0.00	0.00	0.00	0.00	0.00	0.00	0.00	0.00	0.00	0.00	0.00
Hg	0.00	0.00	0.00	0.00	0.00	0.00	0.00	0.00	0.00	0.00	0.00	0.00	0.01	0.01	0.01	0.00
Pb	0.90	0.96	0.00	0.00	0.00	0.00	0.00	0.00	0.00	0.00	5.40	5.35	8.70	8.26	0.00	0.00
Sb	0.00	0.00	0.01	0.00	0.00	0.01	0.00	0.00	0.00	0.00	3.96	4.07	11.08	11.49	4.24	4.18
As	0.00	0.00	0.32	0.01	0.01	0.91	0.00	0.01	0.00	0.00	0.00	0.00	0.00	0.00	0.07	0.09
Bi	0.00	0.01	0.00	0.00	0.00	0.00	0.00	0.00	0.00	0.00	0.07	0.07	0.12	0.12	0.01	0.00
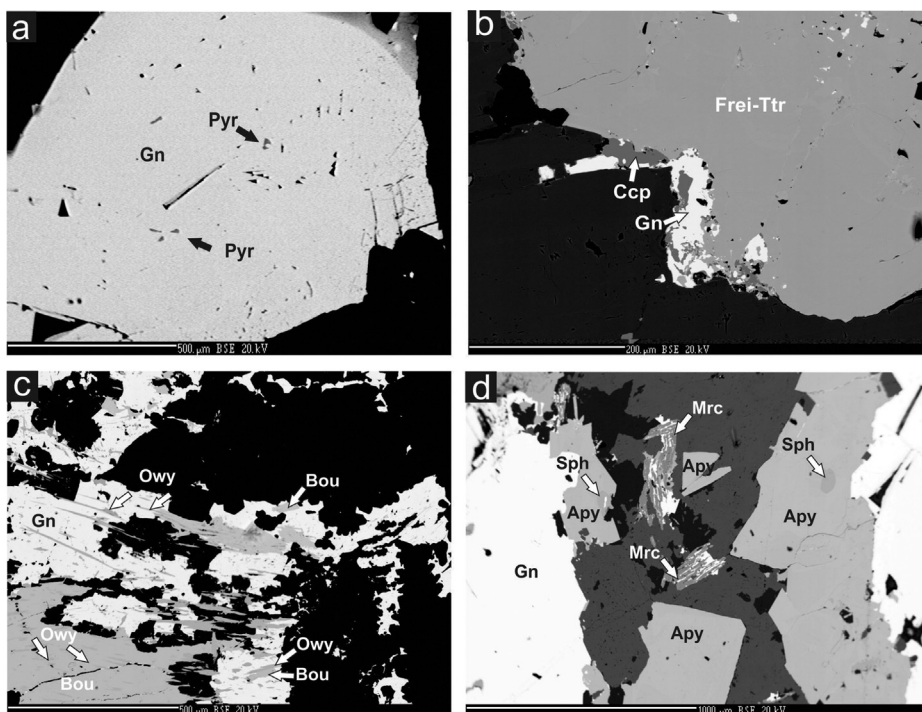
Fig. 3. Back-scattered electron images. A. Pyrargyrite (Pyr) inclusions in galena. B. Mineral of the freibergite–tetrahedrite series (Frei-Ttr) with different shades of gray due to the variable contents of Ag along the crystal that replaces galena (Gn) and chalcopyrite (Ccp). C. Boulangerite (Boul) and owyheeite (Owy) replacing galena. D Marcasite (Mrc) in fine aggregates with banded texture and arsenopyrite (Apy) in quartz gangue.
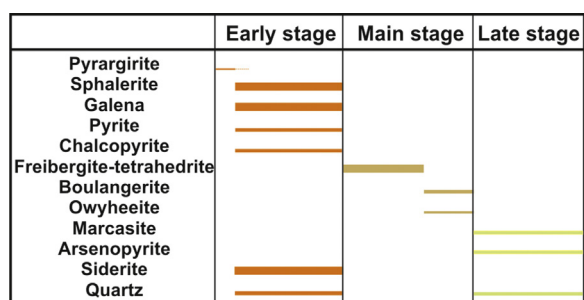
Fig. 4. Paragenetic sequence of the Paramillos de Uspallata deposit. The width of the bars indicates the relative abundance of the ore minerals.

isotopes at the Department of Mineralogy, University of Geneva, Switzerland, using a ThermoTRITON mass spectrometer. Lead isotope ratios were corrected for instrumental fractionation by a factor of 0.07% per a.m.u. based on more than 90 measurements of the SRM981 standard and using the standard values of Todt et al. (1984). The external reproducibility of the standard ratios was 0.11% for $^{206}Pb/^{204}Pb$, 0.12% for $^{207}Pb/^{204}Pb$, and 0.20% for $^{208}Pb/^{204}Pb$. Additionally, one galena sample from another vein was analyzed for Pb isotopes at the ACTLABS Laboratories, Canada, with a Finnigan MAT–261 multi-collector mass spectrometer. Lead isotope ratios were corrected for mass fractionation calculated from replicate measurements of Pb isotope composition in NBS SRM–982 standards. The external reproducibility of the standard ratios was 0.1% for $^{206}Pb/^{204}Pb$ and $^{207}Pb/^{204}Pb$ and 0.2% for $^{208}Pb/^{204}Pb$.

The lead isotope composition of galena was found to be variable in $^{206}Pb/^{204}Pb$ (18.4239 to 18.5012) and $^{208}Pb/^{204}Pb$ (38.2470 to 38.3192) and different from that of the basaltic host rock (Table 3). In the plumbotectonic diagrams (Fig. 5a and b), the lead from the galena plots very close to the orogen curve.

5. Discussion

5.1. The descriptive model

The features of the Paramillos de Uspallata vein-type deposit described above plus information provided by

previous work were used to outline a new descriptive model (see below).

5.1.1. Age of the mineralization and tectonic setting

Since there are no geochronological data of the Paramillos de Uspallata deposit, the relative age of the mineralization is constrained from field relationships. Mineralized vein strikes are mainly coincident with the NW and WNW normal and sinistral strike-slip faults of Triassic age recognized in the north-central part of the Cuyo Basin (Giambiagi et al., 2011). No crosscutting relations between the Paramillos de Uspallata veins and the Miocene volcanics of the area have been reported, and the veins are cut by north–south thrusts linked to the Andean deformation, which, at that latitude, started by the middle Miocene (Ramos et al., 2002). Based on the age of the host rocks and the structural controls, the deposit could be considered approximately as Middle to Late Triassic and thus contemporaneous with rifting development. In this extensional tectonic setting, the volcanics of the synrift sequence attained sub-greenschist metamorphism (prehnite–pumpellyite facies, ~250–350 °C) as a result of crustal thinning and raised thermal gradients (diastathermal metamorphism), as proposed for the Mesozoic Neuquén Rift Basin located further south (Rubinstein et al., 2007).

5.1.2. Ore paragenesis and metal ratios

Three stages of mineralization can be recognized at the Paramillos de Uspallata vein deposit (Fig. 4). The early stage consists mainly of Pb–Zn–(Cu) sulfides and has very low Ag contents. The main mineralization stage is composed of Ag–Cu and Pb–(Ag) Sb-bearing sulfosalts and is followed by a late barren stage.

Paragenesis consisting of galena and sphalerite with minor pyrite and chalcopyrite along with diverse sulfosalts, including (Ag)-tetrahedrite and silver minerals in a dominantly siderite and/or quartz gangue, typically occurs in CSS Pb–Zn–Ag veins (see Beaudoin and Sangster, 1992) and particularly in those associated with rift tectonic settings, e.g., base metal veins of the Purcell Basin (Paiement et al., 2012), High Atlas Range (Bouabdellah et al., 2009) and Mesozoic Aulus basin (Munoz et al., 2016).

Table 2

Oxygen and carbon isotope compositions of quartz and siderite from different veins of the Paramillos de Uspallata deposit. The isotope fractionation in fluids was calculated according to Sharp et al. (2016), Zheng (1999) and Golyshev et al. (1981) at 190 °C and 210 °C respectively (statistical mode temperatures from Garrido et al., 2001).

Vein	$\delta^{18}O$ SMOW quartz	$\delta^{18}O$ SMOW fluid (quartz)	$\delta^{18}O$ SMOW siderite	$\delta^{18}O$ SMOW fluid (siderite)	$\delta^{13}C$ PDB siderite	$\delta^{13}C$ PDB fluid (siderite)
Belén	14.21	1.711; 3.015				
Mendoza	15.25	2.739; 4.043				
San Lorenzo	16.52	3.993; 5.299				
San Miguel	16.16	3.637; 4.943				
Santa Rita	16.2	3.677; 4.983				
San Pedro			20.84	9.067; 10.278	−2.97	−6.255; −5.559
Tajo (1)[a]	13.2	0.714; 2.016	19.1	7.347; 8.556		
Tajo (2)[a]	12.3	−0.175; 1.126	16.3	4.579; 5.785		
Tajo (3)[a]	11.5	−0,965; 0,334	18.4	6.655; 7.863		
Tajo (4)[a]	13.8	1.306; 2.609	17.4	5.666; 6.873		

[a] Data from Garrido et al. (2001).

Table 3

Lead isotope compositions of galena from different Paramillos de Uspallata veins and the Triassic host rock basalts (whole rock) corrected to 235 Ma.

Vein	$^{206}Pb/^{204}Pb$	$^{207}Pb/^{204}Pb$	$^{208}Pb/^{204}Pb$
Vallejos	18.497	15.587	38.303
San Miguel	18.424	15.581	38.247
Florida	18.501	15.587	38.319
Tajo	18.485	15.564	38.247
Basalt	$^{206}Pb/^{204}Pb$	$^{207}Pb/^{204}Pb$	$^{208}Pb/^{204}Pb$
1	18.6859	15.599	38.5119
2	18.6229	15.6029	38.4630

Although the Paramillos de Uspallata deposit has Ag/Ag + Pb ($\sim$0.65) similar to that of CSS Pb–Zn–Ag veins (0.22–0.63), it has a lower Pb/Pb + Zn ($\sim$0.42) than this type of deposits (0.51–0.72) (see Beaudoin and Sangster, 1992).

5.1.3. Physico-chemical conditions and origin of the hydrothermal fluids

According to Garrido et al. (2001), the early-stage mineralizing fluids had temperatures between 160° and 250 °C and salinities that ranged from $\sim$4 to 19 wt% NaCl eq., and probably carried Mg and Ca. Moreover, the 1.47–14.54 mole percent FeS in sphalerite (see sphalerite composition in Table 1) indicates an intermediate (although variable) sulfidation state for the mineralizing fluids (see Einaudi et al., 2003, and references therein). Besides, the oxygen and carbon isotope composition of the Paramillos de Uspallata gangue minerals is consistent with a magmatic or metamorphic origin for the early stage mineralizing fluids which were mixed with varying proportions of meteoric fluids during the late hydrothermal barren stage.

Around the world, CSS Pb–Zn–Ag veins derive from mixed deep-seated (metamorphic) and meteoric fluids that have a wide range of temperatures (170 to 450 °C) and variable (up to 26%), but characteristically moderate salinities (see Beaudoin and Sangster, 1992). The mineralizing fluids of the Paramillos de Uspallata deposit are within the range of temperature and salinity of the CSS Pb–Zn–Ag deposit. However, although a metamorphic origin of the fluids is consistent with the geodynamic scenario of diastathermal metamorphism associated with the formation of the Cuyo rift basin, the involvement of magmatic fluids in their genesis cannot be ruled out.

5.1.4. Sources of the sulfur and lead

The $\delta^{34}S_{H_2S}$ values for reduced sulfur calculated from the isotopic composition of sphalerite and galena obtained by Garrido et al. (2001) using the equations of Li and Liu (2006) in the sphalerite homogenization temperature range (180 °C–225 °C, see Garrido et al., 2001) vary between 2.2‰ and 11.1‰. This range, which is close to that of the magmatic field (generally between –5 and 7‰, see Seal II, 2006) suggests the involvement of magmatic sulfur, either derived from magmatic fluids and/or leached from the host volcano-sedimentary sequence. The sulfur isotopic composition in different CSS Pb–Zn–Ag veins suggests that it derived from the leaching of the local country rocks or the thermochemical reduction of marine sulfate (e.g., Beaudoin and Sangster, 1992; Bouabdellah et al., 2009; Paiement et al., 2012).

The Pb isotope ratios obtained for galena from different veins of the Paramillos de Uspallata deposit are distinctly lower than those of the host basalts, indicating the involvement of an older (and less radiogenic) source for this metal. In the plumbotectonic diagrams, the samples plot in a range between 320 and 260 Ma (see Fig. 4), which allows suggesting that the arc Permian volcanics of the Choiyoi Group and the underlying Carboniferous marine sedimentary rocks that form the Paleozoic basement of the Cuyo Basin (Cortés et al., 1997; Spalletti, 1999) are possible sources of lead. Moreover, the samples plot between the mantle and the orogen evolution curve, but very close to the latter, as it happens with the Choiyoi volcanics and the genetically related ore deposits (Rubinstein et al., 2004). This is consistent with the Pb isotope mixture signature of the CSS Pb–Zn–Ag veins in which Pb derives from a mixture of rocks that have been stored for a long time in the upper crust and rocks deformed during different orogenic cycles and also with a contribution of Pb from the lower crust and the mantle (Beaudoin and Sangster, 1992; Paiement et al., 2012). Moreover, the lead isotopic composition of galena from the Paramillos de Uspallata plots in the field of the Mesozoic deposits from the Purcell Basin and Coeur d'Alene deposits (Fig. 6), which defines an
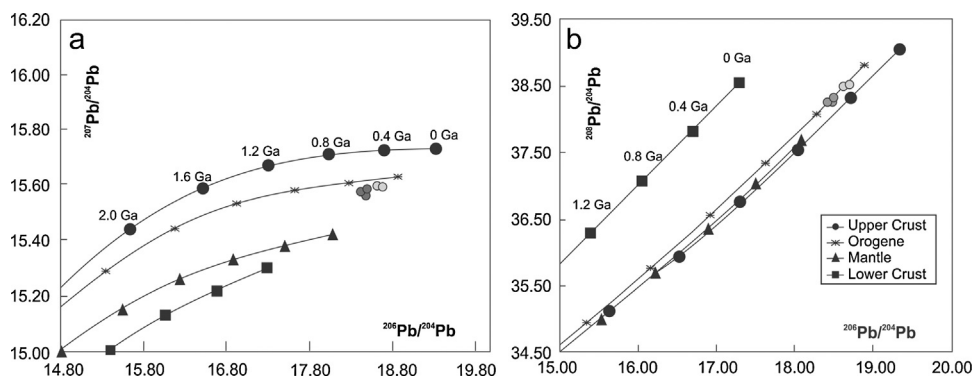
Fig. 5. Uranogenic (a) and thorogenic (b) Pb isotope diagrams showing the plumbotectonic curves of Zartman and Doe (1981) and the Paramillos de Uspallata galena composition (gray circles).
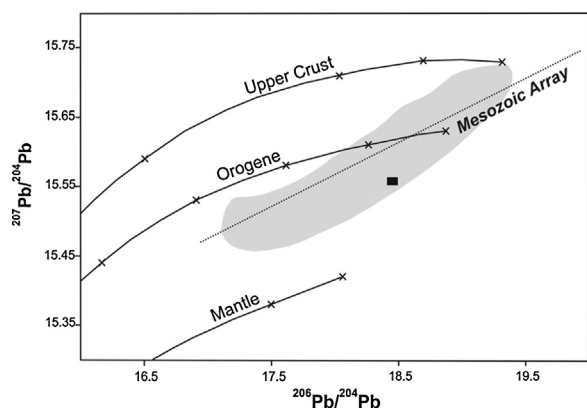
Fig. 6. $^{207}Pb/^{204}Pb$ vs. $^{206}Pb/^{204}Pb$ diagram showing the Mesozoic deposits from the Purcell Basin and Coeur d'Alene district (gray field) and the Paramillos de Uspallata deposit (black field). Modified from Paiement et al. (2012).

array resulting from several lead-mixing events during the Mesozoic–Cenozoic tectonics (Paiement et al., 2012).

5.1.5. The genetic model

Based on the ore and gangue mineralogy and particularly the proximity to the Cu–Mo porphyry and Au-epithermal deposits, Garrido et al. (2001) classified the Paramillos de Uspallata Pb–Zn–Ag veins as a carbonate-base metal and gold system associated with the Miocene porphyry-type deposits of the area (i.e. Cordilleran polymetallic mineralization). However, the stratigraphic relationships and the structural controls clearly contradict this hypothesis. Moreover, the Paramillos de Uspallata Pb–Zn–Ag veins do not display the characteristic base metal zonation (Cu → Zn; Pb → Ag) typical of the Cordilleran veins (Catchpole et al., 2015).

Bearing in mind its tectonic scenario, the Paramillos de Uspallata deposit could be considered as a "detachment-related mineralization". This deposit model, which was defined by Long (1992) and later expanded by Zappettini et al. (2017), includes Mn bedded and vein deposits, Ba–F veins, Cu–Fe–Pb–Ag–Au replacement and veins, five-element veins, Se-rich polymetallic veins, and Pb–Ag–Zn simple veins. In this model, detachment faults in extensional settings separate an upper cold block with listric and flat normal faults from a lower hot block affected by a metamorphism process. This promotes the circulation of basin brines along the detachment faults toward the normal faults, where they mix with meteoric waters and, under favorable physico-chemical conditions, lead to the deposition of the metals formerly leached from the basin sequence.

The Paramillos de Uspallata deposit is linked to the extensional tectonics that followed the collapse of the Permian orogen and resulted in a rift formation and the consequent rise of the asthenospheric mantle and diasta-thermal metamorphism that would have triggered the hydrothermal system. Although the results of stable isotopes are consistent with a mixture source of metamorphic and meteoric origin for the mineralizing fluids as in the detachment-related deposits (Zappettini et al., 2017),

the involvement of magmatic fluids (and sulfur) cannot be ruled out.

6. Conclusions

The metallogenic analysis of the Paramillos de Uspallata vein deposit shows that this deposit is the result of an early Pb–Zn mineralization stage followed by a Ag–Cu–Pb stage and a late barren stage. The hydrothermal fluids had low temperature, low to moderate salinity, and intermediate sulfidation conditions, and probably resulted from a mix between fluids of metamorphic and meteoric origin. However, the contribution of magmatic fluids cannot be precluded. The most suitable source of lead is the upper Paleozoic basement of the Cuyo Basin, whereas the sulfur derived from magmatic fluids and/or leached from the host volcano-sedimentary sequence.

These characteristics allow describing Paramillos de Uspallata as a CSS Pb–Zn–Ag vein deposit genetically linked to the Cuyo rift basin and therefore redefining it as a detachment-related mineralization. Although this genetic model proposes a mixture of metamorphic and meteoric sources for the mineralizing fluids, the involvement of magmatic fluids cannot be ruled out.

References

Barredo, S., 2012. Geodynamic and tectonostratigraphic study of a continental rift: The Triassic Cuyana basin, Argentina. In: Sharkov, E. (Ed.), Tectonics recent advances. InTech Publisher, pp. 99–130.

Baumann, L., 1994. The vein deposit of Freiberg, Saxony. In: Von Gehlen, K., Klemm, D.D. (Eds.), Monograph Series on Mineral Deposits 31. Mineral deposits of the Erzgebirge/Krusné hory, Germany/Czech Republik, pp. 149–167.

Beaudoin, G., Sangster, D.F., 1992. A descriptive model for silver-lead-zinc veins in clastic metasedimentary terranes. Econ. Geol. 87, 1005–1021.

Bouabdellah, M., Beaudoin, G., Leach, D.L., Grandia, F., Cardellach, E., 2009. Genesis of the Assif El Mal Zn–Pb (Cu, Ag) vein deposit. An extension-related Mesozoic vein system in the High Atlas of Morocco. Structural, mineralogical, and geochemical evidence. Mineral. Deposita 44, 689–704.

Brea, M., Artabe, A.E., Spalletti, L.A., 2009. Darwin Forest at Agua de la Zorra: the first in situ forest discovered in South America by Darwin, 1835. Rev. Assoc. Geol. Argent. 64, 21–31.

Carrasquero, S.I., Rubinstein, N.A., Gómez, A., Chiaradia, M., Fontignie, D., Valencia, V., 2017. New insights into the petrogenesis of Miocene magmatism associated with porphyry copper deposits of the Andean Pampean flat slab, Argentina. Geosci. Frontiers https://doi.org/10.1016/j.gsf.2017.10.009.

Carrasquero, S.I., Rubinstein, N.A., Fontignie, D., 2011. Adakite-like signature in volcanic rocks associated with the Oro del Sur Au–(Cu)

epithermal deposit, southern Precordillera, Argentina. Neues Jahrbuch Geol. Paläontol. 26, 309–320.

Catchpole, H., Kouzmanov, K., Putlitz, B., Hun Seo, J., Fontboté, L., 2015. Zoned base metal mineralization in a porphyry system: Origin and evolution of mineralizing fluids in the Morococha District. Peru. Econ. Geol. 110, 39–72.

Clayton, R.N., Mayeda, T.K., 1963. The use of bromide pentafluoride in the extraction of oxygen from oxides and silicates for isotopic analysis. Geochim. Cosmochim. Acta 27, 43–52.

Cortés, J.M., González Bonorino, M., Koukharsky, M., Pereyra, F.X., Brodkorb, A., 1997. Hoja Geológica 3369-09, Uspallata, provincia de Mendoza. Servicio Geológico Minero Argentino, Buenos Aires, 165 p.

Einaudi, M.T., Hedenquist, J.W., Inan, E.E., 2003. Sulfidation state of fluids in active and extinct hydrothermal systems: transitions from porphyry to epithermal environments. In: Simmons, S.F., Graham, I. (Eds.), Volcanic, Geothermal and Ore Forming Fluids: Rulers and Witnesses Processes within the Earth. Society of Economic Geologists Spec. Publ. 10, pp. 285–313.

Fleck, R.J., Criss, R.E., Eaton, G.F., Cleland, R.W., Wavra, C.S., Bond, W.D., 2002. Age and origin of base and precious metal veins of the Coeur d'Alene mining district, Idaho. Econ. Geol. 97, 23–42.

Garrido, M., Domínguez, E., Schalamuk, I., 2001. Veta Tajo, Paramillos de Uspallata, Mendoza. Características del sistema hidrotermal. Rev. Assoc. Geol. Argent. 56, 99–110.

Giambiagi, L., Mescua, J., Bechis, F.A., Martínez, Folguera, A., 2011. Pre-Andean deformation of the Precordillera southern sector, southern Central Andes. Geosphere 7, 219–239.

Golyshev, S.I., Padalko, N.L., Pechenkin, S.A., 1981. Fractionation of stable oxygen and carbon isotopes in carbonate systems. Geochem. Int. 18, 85–99.

Kay, S.M., Mpodozis, C., 2002. Magmatism as a probe to the Neogene shallowing of the Nazca plate beneath the modern Chilean flat-slab. J. S. Am. Earth Sci. 15, 39–57.

Kay, S.M., Mpodozis, C., Ramos, V., Munizaga, F., 1991. Magma source variations for Mid–Late Tertiary magmatics rocks associated with a shallowing subduction zone and a thickening crust in the central Andes (28° to 33°S). In: Harmon, R., Rapela, C.W. (Eds.), Andean Magmatism and its Tectonic Setting. Geol. Soc. America Spec. Paper 265, Boulder, CO, USA, pp. 113–137.

Lawrence, L.J., 1962. Owyheeite from Rivertree, New South Wales. Mineral. Mag. 33, 315–319.

Lavandaio, E., Fusari, C., 1999. Distrito polimetálico Mendoza Norte, Mendoza. In: Zappettini, E. (Ed.), Recursos Minerales de la República Argentina. Servicio Geológico Minero Argentino, Anales 35, Buenos Aires, pp. 1705–1716.

Leach, D.L., Hofstra, A.H., Church, S.E., Snee, L.W., Vaughn, R.B., Zartman, R.E., 1998. Evidence for Proterozoic and Late Cretaceous-Early Tertiary ore-forming events in the Coeur d'Alene district, Idaho and Montana. Econ. Geol. 93, 347–359.

Legarreta, L., Uliana, M.A., 1996. The Jurassic succession in West–Central Argentina: Stratal pattern, sequences and paleogeographic evolution. Palaeogeogr. Palaeoclimatol. Palaeoecol. 120, 303–330.

Li, Y.B., Liu, J.M., 2006. Calculation of sulfur isotope fractionation in sulfides. Geochim. Cosmochim. Acta 70, 1789–1795.

Long, K.R., 1992. Descriptive model of detachment-fault-related mineralization. In: Bliss, J. (Ed.), Developments in Mineral Deposit Modeling. U.S. Geol. Surv. Bull. 2004, pp. 57–62.

Lüders, V., Möller, P., 1992. Fluid evolution and ore deposition in the Harz Mountains, Germany. Eur. J. Min. 4, 1053–1068.

Lydon, J.W., 2007. Geology and metallogeny of the Belt-Purcell basin. In: Goodfellow, W.D. (Ed.), Mineral Deposits of Canada: A Synthesis of Major Deposit-Types, District Metallogeny, the Evolution of Geological Provinces, and Exploration Methods. Geol. Assoc. Canada, Mineral Deposits Division, Spec. Publ. 5, pp. 581–607.

Lynch, J.V.G., Longstaffe, F.J., Nesbitt, B.E., 1990. Stable isotopic and fluid inclusion indications of large-scale hydrothermal paleoflow, boiling, and fluid mixing in the Keno Hill Ag-Pb-Zn district, Yukon Territory, Canada. Geochim. Cosmochim. Acta 54, 1045–1059.

Massabie, A.C., 1986.In: Filón Capa Paramillos de Uspallata, su caracterización geológica y edad, Paramillo de Uspallata, Mendoza, Proceedings 1° Jornadas sobre Geología de Precordillera, San Juan, Argentina, pp. 325–330.

Moëlo, Y., Mozgova, N., Picot, P., Bortnikov, N., Vrublevskaya, Z., 1984. Cristallochimie de l'owyheeite : nouvelles données. Tscherm. Mineral. Petr. Mitt. 32, 271–284.

Munoz, M., Baron, S., Boucher, A., Beziat, D., Salvi, S., 2016. Mesozoic vein-type Pb–Zn mineralization in the Pyrenees: Lead isotopic and fluid inclusion evidence from the Les Argentieres and Lacore deposits. C. R. Geoscience 348, 322–332.

Navarro, H., 1972.In: Área de reserva N° 3. Zona ''Paramillos Norte'', provincia de Mendoza, Proceedings 4° Jornadas Geológicas Argentinas 3, Mendoza, Argentina, pp. 105–125.

Paiement, J.P., Beaudoin, G., Paradis, S., Ullrich, T., 2012. Geochemistry and Metallogeny of Ag-Pb-Zn Veins in the Purcell Basin, British Columbia. Econ. Geol. 107, 1303–1320.

Ramos, V.A., Kay, S.M., 1991. Triassic rifting and associated basalts in the Cuyo Basin, central Argentina. In: Harmon, R.S., Rapela, C.W. (Eds.), Andean Magmatism and its Tectonic Setting. Spec. Pap. 265. Geol. Soc. Am., Boulder, CO, USA, pp. 79–91.

Ramos, V.A., Cristallini, E.O., Perez, D.J., 2002. The Pampean flat-slab of the Central Andes. J. S. Am. Earth Sci. 15, 59–78.

Rayces, E.C., 1949. Informe geológico-minero sobre el mineral del Paramillo de Uspallata. Dirección General de Fabricaciones Militares, Servicio Geológico Minero Argentino, Buenos Aires, unpublished report.

Riley, J.F., 1974. The tetrahedrite–freibergite series, with reference to the Mount Isa Pb–Zn–Ag Orebody. Mineral. Deposita 9, 117–124.

Rocher, S., Abarzúa, F., Tapia Baldis, C., López, M.G., 2015. Volcanism of the Triassic Cuyo Basin in the Calingasta–Barreal Valley, western Argentina. Acta Geol. Lilloana 28 (Suplement), 163–169.

Rubinstein, N., Bevins, R., Robinson, D., Sruoga, P., 2007. Very low grade metamorphism in the Precuyano Unit, Neuquén Basin, Argentina, in: Abstracts of the 20th Colloquium on Latin American Earth Sciences. Kiel, Germany.

Rubinstein, N., Ostera, H., Mallimacci, H., Carpio, F., 2004. Lead isotopes from Gondwanic ore polymetallic vein deposits, San Rafael Massif, Argentina. J. S. Am. Earth Sci. 16, 595–602.

Seal II, R.R., 2006. Sulfur isotope geochemistry of sulfide minerals. Rev. Mineral. Geochem. 61, 633–677.

Segal, S., Godeas, M., Pezzutti, N., Zappettini, E.O., 1999. Distrito de plomo, cinc y plata, Pumahuasi, Jujuy. In: Zappettini, E.O. (Ed.), Recursos Minerales de la República Argentina. Servicio Geológico Minero Argentino, Anales 35, Buenos Aires, pp. 493–497.

Sharp, Z.D., Gibbons, J.A., Maltsev, O., Atudorei, V., Pack, A., Sengupta, S., Shock, E.L., Knauth, L.P., 2016. A calibration of the triple oxygen isotope fractionation in the SiO$_2$.H$_2$O system and applications to natural samples. Geochim. Cosmochim. Acta 186, 105–119.

Spalletti, L.A., 1999. Cuencas triásicas del Oeste Argentino: origen y evolución. Acta Geol. Hispánica 32, 29–50.

Spalletti, L.A., Fanning, C.M., Rapela, C.W., 2008. Dating the Triassic continental rift in the southern Andes: the Potrerillos Formation, Cuyo Basin, Argentina. Geol. Acta 6, 267–283.

Tankard, A.J., Uliana, M.A., Welsink, H.J., Ramos, V.A., Turic, M., Franca, A.B., Milani, E.J., de Brito Neves, B.B., Skármeta, J., Santa Ana, H., Wiens, F., Cirbián, M., López-Paulsen, O., Germs, G.J.B., De Wit, M.J., Machacha, T., McG Miller, R., 1995. Structural and tectonic controls of basin evolution in southwestern Gondwana during the Phanerozoic. In: Tankard, A.J., Suárez, S., Welsink, H.J. (Eds.), Petroleoum basins of South America. Am. Assoc. Petroleum Geol. Mem. 62, pp. 5–52.

Taylor Jr., H.P., 1974. The application of oxygen and hydrogen isotope studies to problems of hydrothermal alteration and ore deposition. Econ. Geol. 69, 843–883.

Todt, W., Cliff, R.A., Hanser, A., Hofmann, A.W., 1984. ^{202}Pb–^{205}Pb spike for Pb isotopic analysis. Abstract Braunlage VIII. Terra Cognita 4 (2), 209.

Uliana, M.A., Biddle, K.T., Cerdan, J., 1989. Mesozoic extension and formation of Argentina sedimentary basin: Extensional tectonics and stratigraphy of the North Atlantic margin. Am. Assoc. Petroleum Geol. Mem. 46, 599–613.

Yáñez, G., Ranero, C., Von Huene, R., Díaz, J., 2001. Magnetic anomaly interpretation across the southern central Andes (32°–34°S): the role of the Juan Fernandez Ridge in the Late Tertiary evolution of the margin. J. Geophys. Res. 106 (B4), 6325–6345.

Zàk, K., Dobes, P., 1991. Stable isotope and fluid inclusions in hydrothermal deposits: The Pribram ore region. Rozpravy Ceskolovenske Akademie Ved, Prague.

Zappettini, E.O., Rubinstein, N., Crosta, S., Segal, S.J., 2017. Intracontinental rift-related deposits: A review of key models. Ore Geol. Rev. 89, 594–608.

Zartman, R.E., Doe, B.R., 1981. Plumbotectonics. Tectonophysics 75, 135–162.

Zheng, Y.F., 1999. Oxygen isotope fractionation in carbonate and sulfate minerals. Geochem. J. 33, 109–126.

Zheng, Y.F., Hoefs, J., 1993. Carbon and oxygen isotopic covariations in hydrothermal calcites. Theoretical modeling on mixing processes and application to Pb–Zn deposits in the Harz Mountains, Germany. Mineral. Deposita 28, 79–89.